Inorganic Chemistry
Article

Inorg. Chem. **2009**, *48*, 10049–10059 **10049**
DOI: 10.1021/ic900727h

Oligonuclear Homoleptic Copper(I) Pyrazolates with Multinucleating Ligand Scaffolds: High Structural Diversity in Solid-State and Solution

Michael Stollenz,† Michael John, Henrike Gehring, Sebastian Dechert, Christian Grosse, and Franc Meyer*

Institut für Anorganische Chemie der Georg-August-Universität Göttingen, Tammannstrasse 4, D-37077 Göttingen, Germany

Received April 14, 2009

The synthesis of three pyrazole-based, potentially binucleating ligands 3,5-bis($R^1N(CH_3)CH_2$)-4-R^2pyrazole (**L**^{1}H: R^1 = pyridyl-2-methyl-, R^2 = Ph; **L**^{2}H: R^1 = 8-quinolyl-, R^2 = H; **L**^{3}H: R^1 = 8-quinolyl-, R^2 = Ph) is described. Reaction of **L**$^{1-3}$H with 1 equiv. of mesitylcopper affords oligonuclear homoleptic complexes of the type $[CuL]_n$ (**1**−**3**). The single crystal X-ray structure of **2** shows a tetranuclear assembly of linear coordinated copper(I)-centers bridged by pyrazolato ligands that alternate above and below the Cu_4 plane, with additional weak interactions from some of the ligand side arms. As the single crystal X-ray structure of **3** reveals, phenyl substitution at the 4-position of the pyrazolato framework leads to significant structural modification of the Cu_4 array, giving a rhombical tetranuclear complex with two linear coordinated copper(I) centers that exhibit a short intramolecular Cu···Cu contact (2.8212(10) Å) and two peripheral copper(I) centers in a distorted tetrahedral coordination mode. Thus, **3** represents a very rare example of an inorganic pyrazolato cuprate which can also be viewed as a partly rearranged structural isomer of **2**. Furthermore, the crystal lattice of **3** shows an extended network of intra- and intermolecular $\pi-\pi$ stacking interactions between the aromatic rings. In solution, **1**−**3** each form two types of oligomers **a** and **b** that slowly (<1 s^{-1}) equilibrate at room temperature. Using Diffusion Ordered Spectroscopy (DOSY) and variable temperature ^{1}H NMR spectroscopy it can be shown that **a** and **b** correspond to a tetrameric and a (planar) trimeric species. Coordination of the pyridyl/quinolyl side arms that is observed in the solid state seems to be only transient in solution.

Introduction

Oligonuclear complexes of monovalent coinage metals in combination with pyrazolate bridging ligands, forming compounds of the general formula $[M(\mu\text{-pz*})]_n$ (pz* = 3,5-substituted pyrazolate, n = 3, 4), have received increasing attention over the past few years. This is not only because of their ability to create unique molecular architectures[1] but also because of their fascinating luminescence properties,[2] their application in homogeneous catalysis,[3] and their potential use as metallomesogens.[4] Furthermore, it was recently shown that Ag(I)[5]- and Au(I)[2d]-pyrazolates bearing electron-withdrawing CF_3-groups in the 3,5-positions serve as π-acidic units to form very interesting supramolecular arene-sandwiched stacks.

Apart from some polymeric coinage metal pyrazolates,[6] most of the structurally elucidated compounds, such as $[M(\mu\text{-}(3,5\text{-}(Ph)_2pz)]_3$ (M = Cu,[7] Ag,[8,9b] Au[9]), $[M(\mu\text{-}(3,5\text{-}(Me)_2pz)]_3$,

*To whom correspondence should be addressed. E-mail: franc.meyer@chemie.uni-goettingen.de. Phone: +49 551 393012. Fax: +49 551 393063.
†Current address: Department of Chemistry, Texas A&M University, P.O. Box 30012, College Station, Texas 77842-3012. E-mail: mstollenz@mail.chem.tamu.edu.

(1) Dias, H. V. R.; Diyabalanage, H. V. K.; Gamage, C. S. P. *Chem. Commun*. **2005**, 1619–1621.
(2) (a) Yang, G.; Raptis, R. G. *Inorg. Chim. Acta* **2003**, *352*, 98–104. (b) Dias, H. V. R.; Diyabalanage, H. V. K.; Rawashdeh-Omary, M. A.; Franzman, M. A.; Omary, M. A. *J. Am. Chem. Soc*. **2003**, *125*, 12072–12073. (c) Kishimura, A.; Yamashita, T.; Aida, T. *J. Am. Chem. Soc*. **2005**, *127*, 179–183. (d) Omary, M. A.; Rawashdeh-Omary, M. A.; Gonser, M. W. A.; Elbjeirami, O.; Grimes, T.; Cundari, T. R.; Diyabalanage, H. V. K.; Gamage, C. S. P.; Dias, H. V. R. *Inorg. Chem*. **2005**, *44*, 8200–8210. (e) Dias, H. V. R.; Diyabalanage, H. V. K.; Eldabaja, M. G.; Elbjeirami, O.; Rawashdeh-Omary, M. A.; Omary, M. A. *J. Am. Chem. Soc*. **2005**, *127*, 7489–7501. (f) Kishimura, A.; Yamashita, T.; Yamaguchi, K.; Aida, T. *Nat. Mater*. **2005**, *4*, 546–549. (g) Ovejero, P.; Mayoral, M. J.; Cano, M.; Lagunas, M. C. *J. Organomet. Chem*. **2007**, *692*, 1690–1697.
(3) (a) Ardizzoia, G. A.; Angaroni, M. A.; La Monica, G.; Cariati, F.; Cenini, S.; Moret, M.; Masciocchi, N. *Inorg. Chem*. **1991**, *30*, 4347–4353. (b) Maspero, A.; Brenna, S.; Galli, S.; Penoni, A. *J. Organomet. Chem*. **2003**, *672*, 123–129.
(4) (a) Barberá, J.; Elduque, A.; Giménez, R.; Oro, L. A.; Serrano, J. L. *Angew. Chem. Int. Ed*. **1996**, *35*, 2832–2835. (b) Barberá, J.; Elduque, A.; Giménez, R.; Lahoz, F. J.; López, J. A.; Oro, L. A.; Serrano, J. L. *Inorg. Chem*. **1998**, *37*, 2960–2967.
(5) Dias, H. V. R.; Gamage, C. S. P. *Angew. Chem. Int. Ed*. **2007**, *46*, 2192–2194.
(6) (a) Ardizzoia, G. A.; Beccalli, E. M.; La Monica, G.; Masciocchi, N.; Moret, M. *Inorg. Chem*. **1992**, *31*, 2706–2711. (b) Masciocchi, N.; Moret, M.; Cairati, P.; Sironi, A.; Ardizzoia, G. A.; La Monica, G. *J. Am. Chem. Soc*. **1994**, *116*, 7668–7676.
(7) Raptis, R. G.; Fackler, J. P., Jr. *Inorg. Chem*. **1988**, *27*, 4179–4182.
(8) Mohamed, A. A.; Pérez, L. M.; Fackler, J. P., Jr. *Inorg. Chim. Acta* **2005**, *358*, 1657–1662.
(9) (a) Raptis, R. G.; Murray, H. H.; Fackler, J. P., Jr. *J. Chem. Soc., Chem. Commun*. **1987**, 737–739. (b) Murray, H. H.; Raptis, R. G.; Fackler, J. P., Jr. *Inorg. Chem*. **1988**, *27*, 26–33.

Published on Web 10/05/2009

Chart 1. Cu(I) and Ag(I) Pyrazolates with Additional N- and S- Donating Side Groups (∩N = 6-methyl-2-pyridyl-)

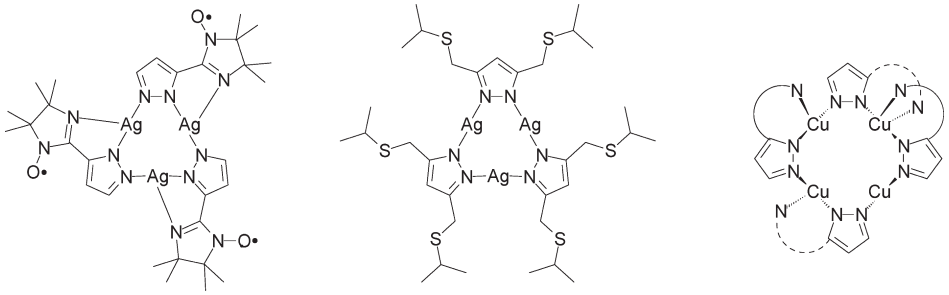

$[M(\mu\text{-}(3,4,5\text{-}(Me)_3pz)]_3$ (M = Cu),[10] $[M(\mu\text{-}3,5\text{-}(Me)_2\text{-}(4\text{-}(NO_2)\text{-}pz)]_3$ (M = Cu),[11] and $[M(\mu\text{-}(3,5\text{-}(F_3C)_2pz)]_3$ (M = Cu, Ag)[12] show a trimeric ring structure, whereas tetrameric arrangements of Cu(I),[3b,13] Au(I),[2a] and, just recently published, Ag(I)[14] pyrazolates, are less common. Well-defined higher oligomers are very rare, only one Au(I)-hexamer has been reported so far.[9]

Although this has not been systematically investigated yet, it seems to be likely that both the radii of the coinage metal ions and the steric bulk of the substituents in the 3,5-positions of the pyrazolate backbone control the nuclearity of these frameworks. While these factors are reasonably understood in case of the parent organic pyrazoles $(pzH)_n$ where aggregation occurs via hydrogen bonding,[15] predictions of the structures of metal-containing pyrazolates are clearly more complicated. On the one hand, interactions between metal centers and donor atoms may play an important role in pre-organizing the oligomeric framework. On the other hand, in case of coinage metals, weak $d^{10}\cdots d^{10}$ contacts may support this pre-organization or the final arrangement itself. Pyrazolate ligands with additional coordinating side groups in their 3,5-positions have received much less attention in this context. This is somewhat surprising, since a variety of bi- and tetranuclear complexes with this type of compartmental ligands[16] have been developed as model compounds and precatalysts for, e.g., biomimetic applications.[17,18] While no example of a corresponding binuclear Cu(I) complex for this type of binucleating ligands has been described in the literature so far, monovalent coinage metal pyrazolates with additional coordinating side groups are promising candidates to form oligonuclear structures differing from the known cyclic trimeric and tetrameric arrays, potentially with interesting material properties. Among the very few examples are Cu(I)- and Ag(I)-pyrazolates with one additional N-donating side group in the 3-position that are shown by their X-ray structures to form trimeric rings (Chart 1).[19] As previously demonstrated by our group, a Ag(I)-pyrazolate with potentially chelating thioether side arms in the 3,5-positions affords also a trimeric structure in the solid state, however, without any involvement of these side groups in metal coordination.[20]

Around ten years ago Stavropoulos and co-workers reported on Cu(I)-pyrazolates based on 2-(3,5)-pyrazolyl)-6-methylpyridine that form not only trimeric rings but also a rare tetranuclear cyclic array (Chart 1). Dimerization of two such Cu_4 cores occurs via an *inter*molecular Cu···Cu contact between two linearly coordinated copper atoms (3.0045(13) Å).[21]

Recently, we reported on a new compartmental pyrazolate-based ligand $\mathbf{L^1}$H bearing additional N-donating side groups in the 3,5-positions that is capable to form a remarkably stable octanuclear σ-mesityl-bridged O-centered cuprocuprate.[22] This complex was derived from a stoichiometric ratio $\mathbf{L^1}$H:"CuMes" of 1:4 and dioxygen.

In view of the interest in and the high potential of homoleptic Cu(I) pyrazolates, we were interested to obtain such compounds from $\mathbf{L^1}$H and, to extend their scope, the new related ligands $\mathbf{L^2}$H and $\mathbf{L^3}$H that bear the more rigid quinolyl side groups. We found $\mathbf{L^{1-3}}$H and "CuMes" (molar ratio 1:1) suitable to afford the corresponding homoleptic copper(I) pyrazolates **1**−**3** in clean reactions under elimination of mesitylene. In this contribution, we present the X-ray structures of the complexes **2** and **3**, together with detailed NMR studies to elucidate their behavior in solution.

Results and Discussion

Synthesis of the Ligands. Starting from 3,5-bis(hydroxymethyl)-4-phenyl-1*H*-pyrazole[23] or 3,5-bis(hydroxymethyl)-1*H*-pyrazole,[24] respectively, and the corresponding secondary

(10) (a) Ehlert, M. K.; Rettig, S. J.; Storr, A.; Thompson, R. C.; Trotter, J. *Can. J. Chem.* **1990**, *68*, 1444–1449. (b) Ehlert, M. K.; Rettig, S. J.; Storr, A.; Thompson, R. C.; Trotter, J. *Can. J. Chem.* **1992**, *70*, 2161–2173.

(11) Ardizzoia, G. A.; Cenini, S.; La Monica, G.; Masciocchi, N.; Maspero, A.; Moret, M. *Inorg. Chem.* **1998**, *37*, 4284–4292.

(12) Dias, H. V. R.; Polach, S. A.; Wang, Z. *J. Fluorine Chem.* **2000**, *103*, 163–169.

(13) (a) Ardizzoia, G. A.; Cenini, S.; La Monica, G.; Masciocchi, N.; Moret, M. *Inorg. Chem.* **1994**, *33*, 1458–1463. (b) Fujisawa, K.; Ishikawa, Y.; Miyashita, Y.; Okamoto, K. *Chem. Lett.* **2004**, *33*, 66–67.

(14) Yang, G.; Raptis, R. G. *Inorg. Chim. Acta* **2007**, *360*, 2503–2506.

(15) Foces-Foces, C.; Alkorta, I.; Elguero, J. *Acta Crystallogr.* **2000**, *B56*, 1018–1028.

(16) Klingele, J.; Dechert, S.; Meyer, F. *Coord. Chem. Rev.* **2009**, DOI: 10.1016/j.ccr.2009.03.026.

(17) (a) Meyer, F.; Pritzkow, H. *Angew. Chem. Int. Ed.* **2000**, *39*, 2112–2115. (b) Ackermann, J.; Meyer, F.; Kaifer, E.; Pritzkow, H. *Chem.—Eur. J.* **2002**, *8*, 247–258. (c) Prokofieva, A.; Prikhod'ko, A. I.; Enyedy, E. A.; Farkas, E.; Maringgele, W.; Demeshko, S.; Dechert, S.; Meyer, F. *Inorg. Chem.* **2007**, *46*, 4298–4307. (d) van der Vlugt, J. I.; Meyer, F. *Top. Organomet. Chem.* **2007**, *22*, 191–240. (e) Prokofieva, A.; Prikhod'ko, A. I.; Dechert, S.; Meyer, F. *Chem. Commun.* **2008**, 1005–1007.

(18) (a) Meyer, F. *Eur. J. Inorg. Chem.* **2006**, 3789–3800. (b) Meyer, F. *Prog. Inorg. Chem.* **2009**, *56*, 487–542.

(19) (a) Singh, K.; Long, J. R.; Stavropoulos, P. *J. Am. Chem. Soc.* **1997**, *119*, 2942–2943. (b) Yamada, S.; Ishida, T.; Nogami, T. *Dalton Trans.* **2004**, 898–903.

(20) Meyer, F.; Jacobi, A.; Zsolnai, L. *Chem. Ber./Recueil* **1997**, *130*, 1441–1447.

(21) Singh, K.; Long, J. R.; Stavropoulos, P. *Inorg. Chem.* **1998**, *37*, 1073–1079.

(22) Stollenz, M.; Grosse, C.; Meyer, F. *Chem. Commun.* **2008**, 1744–1746.

(23) Sachse, A.; Penkova, L.; Noël, G.; Dechert, S.; Varzatskii, O. A.; Fritsky, I. O.; Meyer, F. *Synthesis* **2008**, *5*, 800–806.

(24) (a) Schenck, T. G.; Downes, J. M.; Milne, C. R. C.; Mackenzie, P. B.; Boucher, H.; Whelan, J.; Bosnich, B. *Inorg. Chem.* **1985**, *24*, 2334–2337. (b) Röder, J. C.; Meyer, F.; Pritzkow, H. *Organometallics* **2001**, *20*, 811–817.

Scheme 1. Synthesis of $\mathbf{L^{1\text{-}3}H}$

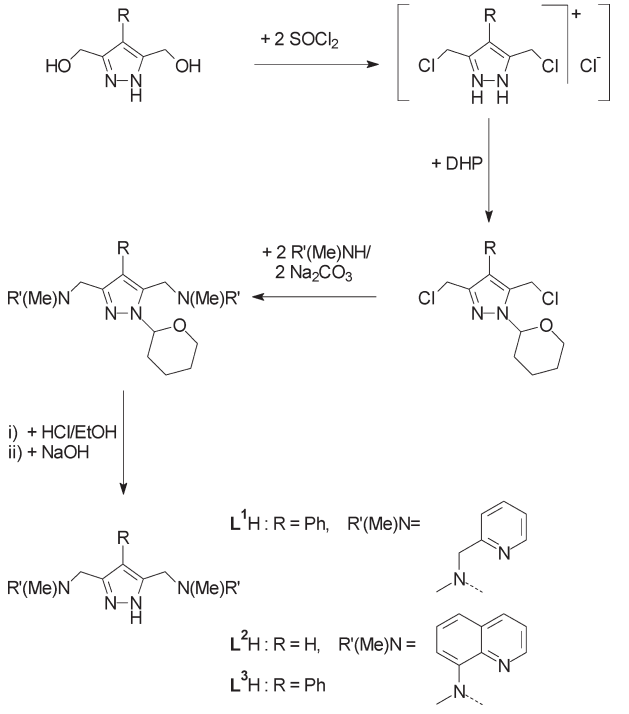

amines, $\mathbf{L^{1-3}H}$ were prepared in four steps (Scheme 1). To prevent side reactions of the nucleophilic pyrazole NH-function, it was protected with dihydropyrane (DHP), a method that was successfully applied in the synthesis of similar pyrazole-based ligands previously described.[24b,25] Aminolysis of the 3,5-bis(chloromethyl)-pyrazole derivatives and subsequent deprotection of the pyrazole NH group by treating with ethanolic HCl gave the desired ligands in overall good yields.

Whereas $\mathbf{L^1H}$ was isolated as a highly viscous, hygroscopic resin, $\mathbf{L^2H}$ and $\mathbf{L^3H}$ could be obtained as colorless to yellow powders after chromatographic workup. Because of the presence of weakly polar side groups like phenyl in the 4-position of the pyrazole-framework and/or the peripheral quinolyl-substituents, all ligands are readily soluble not only in CH_2Cl_2 and tetrahydrofuran (THF) but also in less polar solvents such as benzene and toluene.

EI mass spectra of the new ligands $\mathbf{L^2H}$ and $\mathbf{L^3H}$ show the molecular ion peaks in good agreement with their calculated isotopic distribution patterns at m/z = 408 and 484, respectively. The ^1H and ^{13}C NMR spectra of both compounds, measured in THF-d_8 at room temperature, display only one set of signals related to the CH_2-(NCH_3)-8-quinolyl side arms and, in case of $\mathbf{L^3H}$, an additional set of aromatic resonances of the phenyl group (see Experimental Section). Apart from the pyrazole NH proton, only the signals assigned to the CH_2 group in $\mathbf{L^2H}$ as well as the CH_2, CH_3 and quinolyl-H^2 protons in $\mathbf{L^3H}$ are somewhat broadened. Hence, in all three compounds, both the pyrazole N−H tautomerism and, despite the bulkiness of the quinolyl and phenyl groups, rotations around the C−C and C−N axes of the 3,5-pyrazole−CH_2(NCH_3) bridges are rather fast.

(25) Röder, J. C.; Meyer, F.; Konrad, M.; Sandhöfner, S.; Kaifer, E.; Pritzkow, H. *Eur. J. Org. Chem.* **2001**, 4479–4487.

Scheme 2. Formation of the Complexes **1**−**3**

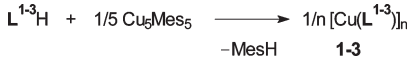

Synthesis of the Complexes. The reaction of $\mathbf{L^{1-3}H}$ with 1 equivalent of mesitylcopper at −78 °C affords mesitylene and light yellow (**1**) or orange to red complexes (**2** and **3**) of the stoichiometric composition $[Cu(\mathbf{L^{1-3}})]_n$ (Scheme 2).

2 and **3** are readily soluble in THF, but only sparingly in benzene and toluene, whereas **1** can be dissolved in all three solvents without difficulties. However, all complexes **1**−**3** are just moderately soluble in diethyl ether and nearly insoluble in non-polar solvents such as pentane. Therefore, crystallization of **1**−**3** was performed by concentrating or layering the reaction solution with diethyl ether to yield the complexes as microcrystalline solids that were washed with pentane to remove the byproduct mesitylene. Despite the presence of oxidizable Cu(I) centers, solid samples of **1**−**3** are resistant to moisture and stable in air for several days. Solutions of **1**−**3**, however, rapidly turn green (**1**) or brown (**2** and **3**) in the presence of air. The FAB-MS spectra of all three complexes are very similar. Thus **1**−**3** exhibit a peak derived from a tetramer (n = 4) that has released one ligand at m/z = 1485.6 (**1**), 1473.5 (**2**), and 1701.5 (**3**), respectively. Furthermore, a corresponding fragment of the composition $[Cu_3(\mathbf{L^{1-3}})_2]^+$ at m/z = 1011.2 (**1**) (**2**: 1003.2, **3**: 1155.2), a dimeric fragment (n = 2) at m/z = 948.3(**1**) (**2**: 940.2, **3**: 1092.2), and the base peak at m/z = 537.1 (**1**) (**2**: 535.0, **3**: 611.0) that is attributed to the binuclear fragment $[Cu_2(\mathbf{L^{1-3}})]^+$, are observed. All experimental isotopic distribution patterns are in good agreement with their corresponding calculated ones.

X-ray Structure Determinations of 2 and 3. Despite several attempts to grow single crystals of complex **1** no crystalline material suitable for X-ray analysis was obtained. However, in case of complex **2**, small orange plates suitable for an X-ray structure determination were isolated from a concentrated solution in toluene at room temperature. Single crystals of **3** suitable for X-ray analysis were obtained as orange needles from a concentrated solution of **3** in toluene at +4 °C. The molecular structures of **2** and **3** are depicted in Chart 2 and Figures 1 and 2.

The molecular structure of **2** is represented by a tetranuclear "tub-shaped" core with bridging heterocyclic rings that alternate above and below the Cu_4-plane. This S_4 symmetric so-called N,N'-exobidentate arrangement of the pyrazolate bridges has been already observed in the few tetranuclear Cu(I)pyrazolates described in the literature so far.[3b,13] In contrast to those structures, each copper atom in **2** is additionally coordinated by the aromatic N-donor of one of the CH_2(N−CH_3)-8-quinolyl side arms that alternate below and above the Cu_4 plane. This bond is relatively weak, but not negligible, as indicated by the Cu1−N4 distances of 2.640(5) Å, while the corresponding Cu1···N3 (amino-N) distances (2.932(5)) are even larger and beyond the bonding range. The second set of CH_2(NCH_3)-8-quinolyl side groups does not participate in any coordinative interaction with the copper(I) centers. This situation gives rise to an overall trigonal distorted T-shape environment at each copper

Chart 2. Solid-State Molecular Structures of **2** and **3**

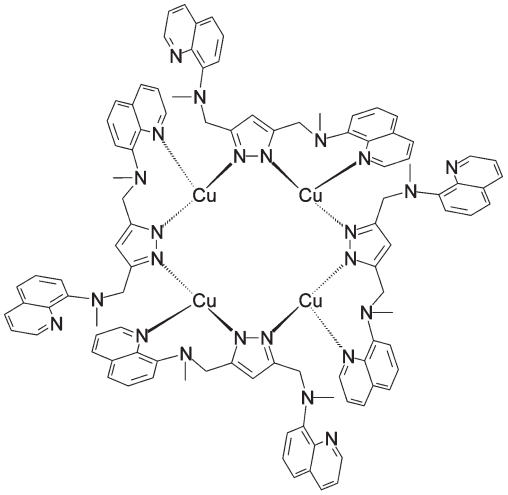

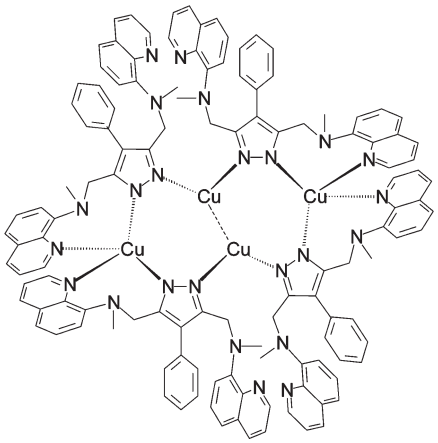

atom, reflected by the bonding angles N1−Cu1−N2′ (170.5(2) Å) and N1−Cu1−N4 (99.92(18) Å), respectively. A comparison of the bonding distances within the tetrameric copper-pyrazolate framework (average Cu−N bond distances 1.868(5) Å) with that of the exterior quinolyl-N-copper bonds clearly demonstrates the inferior role of the third N−donor atom in stabilizing the central copper-pyrazolate core.

A similar situation is observed in the complex [Cu(μ-2-(3(5)-pz,6-Mepy)]$_4$, where the Cu atom is found much closer to the pyrazolate (averaged Cu−N(pyrazolate) distances: 1.885(4) Å) than to the pyridyl substituent (2.297(5)−2.416(5) Å).[21] This underlines the strong σ-donor properties of the N-atoms of the pyrazolate backbone, which in combination with the propensity of copper(I) for 2-fold (linear) coordination serves as dominant driving force for stabilizing the cyclic copper-pyrazolate scaffold. Direct contacts between the copper centers as additional support of the copper-pyrazolate framework can be excluded, since the interatomic Cu···Cu distances in **2**, ranging from 3.434(1) to 4.837(1) Å, are too large for a typical d^{10}−d^{10} bonding interaction.[26]

(26) (a) Jansen, M. *Angew. Chem., Int. Ed. Engl.* **1987**, *26*, 1098–1110. (b) Pyykkö, P. *Chem. Rev.* **1997**, *97*, 597–636.

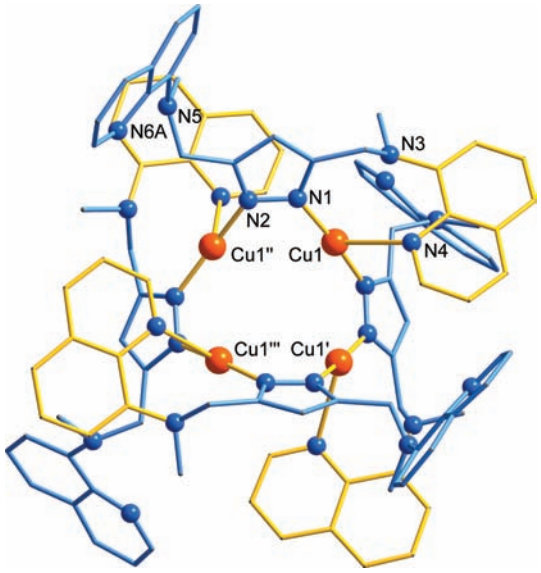

Figure 1. Molecular structure of complex **2**. Hydrogen atoms have been omitted for clarity. Selected interatomic distances (Å) and bond angles (deg): Cu1−N1 1.866(5), Cu1−N2′ 1.870(5), Cu1−N4 2.640(5), Cu1···N3 2.932(5), Cu1···Cu1″ 3.434(1), Cu1···Cu1‴ 4.837(1), N1−N2 1.383(6); N1−Cu1−N2′ 170.5(2), N1−Cu1−N4 99.92(18), N2′−Cu1−N4 89.39(19).

As shown in Figure 2 (see also Chart 2), the molecular structure of **3** exhibits again a tetranuclear cyclic array that is, however, remarkably different to that of **2**. As in **2**, only one of the $CH_2(NCH_3)$-8-quinolyl side arms per ligand molecule is involved in Cu coordination, but in contrast to **2**, each two of the coordinating side arms bind to the same Cu atom. Thus, the structure of **3** contains two fundamentally different sets of copper centers: two peripheral Cu atoms (Cu1 and Cu4) adopt a distorted tetrahedral coordination geometry whereas two central Cu atoms (Cu2 and Cu3) are nearly linearly coordinated by two pyrazolate-N donors (N14−Cu2−N33 = 176.7(2)°, N04−Cu3−N23 = 175.4(2)°). Here, the latter show a short *intramolecular* Cu···Cu contact with a distance of only 2.8212(10) Å, which is close to the sum of two van der Waals radii (2.8 Å)[27] and much shorter than the Cu···Cu distances reported for the copper(I) pyrazolates [Cu(μ-2-(3(5)-pz,6-py)]$_3$ (2.905(3) Å) and [Cu(μ-2-(3(5)-pz,6-Mepy)]$_4$ (3.0045(13) Å).[19a,21] It should be noted that those copper(I) pyrazolates reported previously exhibit exclusively *intermolecular* Cu···Cu contacts which are also known for pyrazolates without any additional donor functionality like [Cu(μ-(3,5-(Me)$_2$-pz)]$_3$ (2.946 Å) and [Cu(μ-(3,4,5-(Me)$_3$pz)]$_3$ (3.069(1) Å).[10] Since the Cu···Cu axis in **3** is almost perpendicular to the N−Cu−N axis (N14−Cu2−Cu3 = 84.10(15)°, N04−Cu3−Cu2 = 96.12(15)°) the overall coordination geometry of Cu2 and Cu3 can again be described as slightly distorted T-shape.

The averaged Cu−N bond lengths of the three-coordinated copper centers (1.858(5) Å) are, within experimental error, identical to those of the corresponding bonds in **2** (1.868(5) Å). However, the Cu−N(pyrazolate) bond distances of the four-coordinated copper centers of **3**, ranging between 1.920(5) and 1.964(5) Å, are

(27) Bondi, A. *J. Phys. Chem.* **1964**, *68*, 441–451.

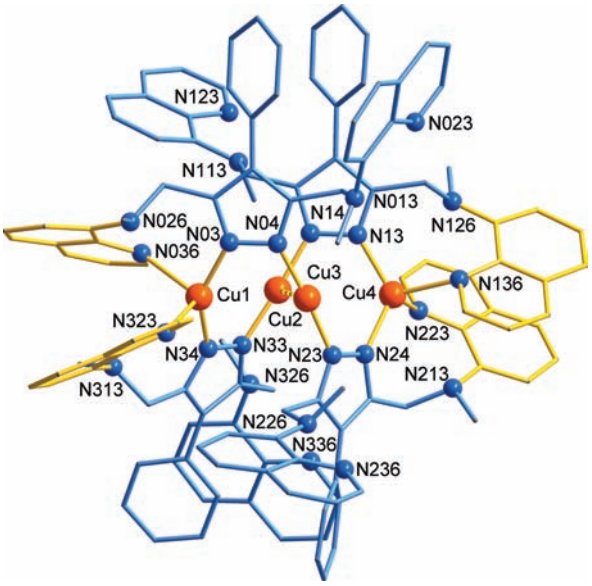

Figure 2. Molecular structure of complex **3**. Hydrogen atoms have been omitted for clarity. Selected interatomic distances (Å) and bond angles (deg): Cu1−N03 1.946(5), Cu1−N34 1.920(5), Cu1−N036 2.477(5), Cu1−N323 2.379(5), Cu1···N026 3.122(5), Cu1···N313 3.139(5), Cu2−N14 1.851(5), Cu2−N33 1.857(5), Cu4−N13 1.959(5), Cu4−N24 1.964(5), Cu4−N136 2.179(5), Cu4−N223 2.188(5), Cu4···N126 3.218(5), Cu4···N213 3.180(5), Cu3−N04 1.867(5), Cu3−N23 1.855(5), Cu2···Cu3 2.8212(10); N03−Cu1−N34 144.26(18), N03−Cu1−N036 97.80(19), N03−Cu1−N323 99.42(19), N34−Cu1−N036 95.87(19), N34−Cu1−N323 104.84(19), N036−Cu1−N323 113.98(17), N14−Cu2−N33 176.7(2), N14−Cu2−Cu3 84.10(15), N33−Cu2−Cu3 96.44(14), N13−Cu4−N24 122.20(17), N13−Cu4−N136 105.8(2), N13−Cu4−N223 109.73(19), N24−Cu4−N136 111.08(19), N24−Cu4−N223 105.7(2), N136−Cu4−N223 100.17(16), N04−Cu3−N23 175.4(2), N04−Cu3−Cu2 96.12(15), N23−Cu3−Cu2 81.72(15).

significantly enlarged, as expected from the higher coordination number. Similar observations were made for the distorted-tetrahedral coordinated copper(I) atoms in $[Cu(\mu\text{-}2\text{-}(3(5)\text{-pz},6\text{-Mepy})]_4$ as well as the organocopper compound $[(\mathbf{L^1}Cu_2(\mu\text{-Mes})_2Cu_2)_2(\mu\text{-O})]$.[21,22] Again, the quinolyl groups seem to be bonded less tightly as indicated by the Cu−N(quinolyl) bond distances (ranging between 2.179(5) and 2.477(5) Å). However, in comparison with **2** (e.g., Cu1−N4 = 2.640(5) Å), these bonds are clearly shorter, whereas the N-donor atoms of the CH_2N-(CH_3) linker are even more distant (3.122(5)−3.218(5) Å) from the copper centers than in **2**.

Interestingly, the crystal packing of **3** exhibits an extended network of intra- and intermolecular $\pi-\pi$ stacking interactions between the copper(I)-coordinating quinolyl side groups. Additional $\pi-\pi$ contacts are also observed between one phenyl group and one non-bonding quinolyl substituent of each complex molecule (Figure 3). Although $\pi-\pi$ stacking is present in the solid-state structure of **2** as well, in this case these interactions should be considered with care, since one quinolyl side group was found to be disordered.

The structural features of individual molecules lead to a remarkable consequence: complex **3** can be viewed as a very rare *inorganic homoleptic cuprate* consisting of two anionic $[Cu(pz)_2]^-$ units, held together by the short

(28) Jastrzebski, J. T. B. H.; van Koten, G. In *Modern Organocopper Chemistry*; Krause, N., Ed.; Wiley VCH GmbH: Weinheim, 2002; pp 1−44.

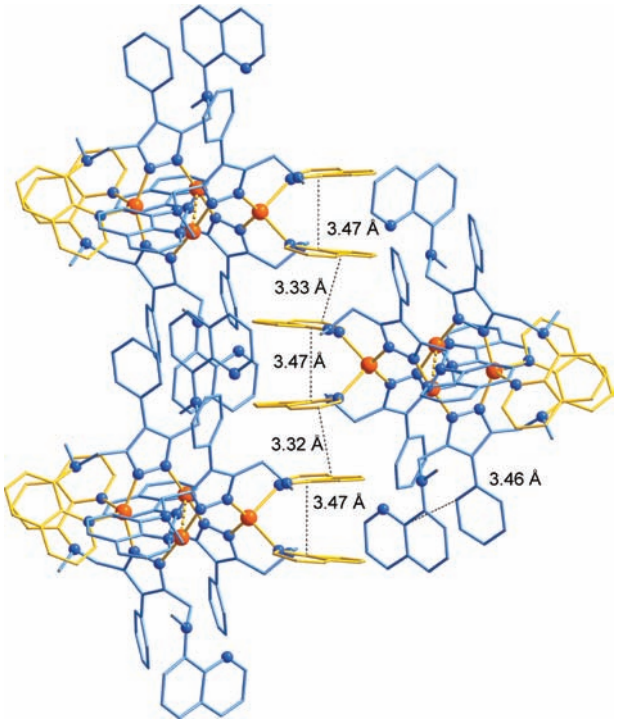

Figure 3. Part of the crystal structure of **3**: representation of three complex molecules within the crystal lattice highlighting intra- and intermolecular $\pi-\pi$ stacking. Close C···C distances are shown exemplarily.

Cu−Cu contact, and two cationic $[Cu(3\text{-}pz(CH_2N\text{-}(CH_3)8\text{-quinolyl})]^+$ parts. Although σ−aryl−bridged organocopper cuprates are well-known,[22,28] the structural characterization of their N-analogous counterparts, for example, those consisting of copper(I) pyrazolates, has received comparably little attention so far. To the best of our knowledge, **3** and $[Cu(\mu\text{-}2\text{-}(3(5)\text{-pz},6\text{-Mepy})]_4$ are the only examples of copper(I)-pyrazolates characterized by an X-ray structure determination that exhibit this remarkable cuprate feature.[21]

Comparison of the solid state structures of **2** and **3** suggests that in solution a smooth interconversion between the two forms should be feasible. The metal ion arrangement in **3** reflects a distortion of the square Cu_4 core of **2** toward a rhomb that brings two opposite copper centers closer together, which is accompanied by interchanging the coordinating and non-coordinating hemilabile quinolyl side arms of two opposite ligands. As such, **3** may be described as an intermediate on the pathway of exchanging the bonding and non-bonding set of hemilabile quinolyl arms of all four ligands around the Cu_4 scaffold (red and blue side arms in Scheme 3). This may proceed via initial (possibly concerted) switching of the coordinating side arms of two opposite ligands concomitant with rhombic distortion of the Cu_4 core, followed by switching the coordinating arms of the two remaining ligands and relaxing of the Cu_4 framework to its square arrangement (Scheme 3). In this picture the potentially chelating ligand side arms give rise to (or accelerate) a new dynamic process of the $(Cu\text{-}pz\text{-})_4$ motif that is not available to related compounds with more simple pyrazolate ligands lacking the functional side arms. It must be noted, however, that this interconversion is not observed directly in solution and may well proceed by a more complex

Scheme 3. Proposed Dynamic Interconversion between Two Indistinguishable Forms of **2** via the Intermediate Species **3** (R = H, Ph)

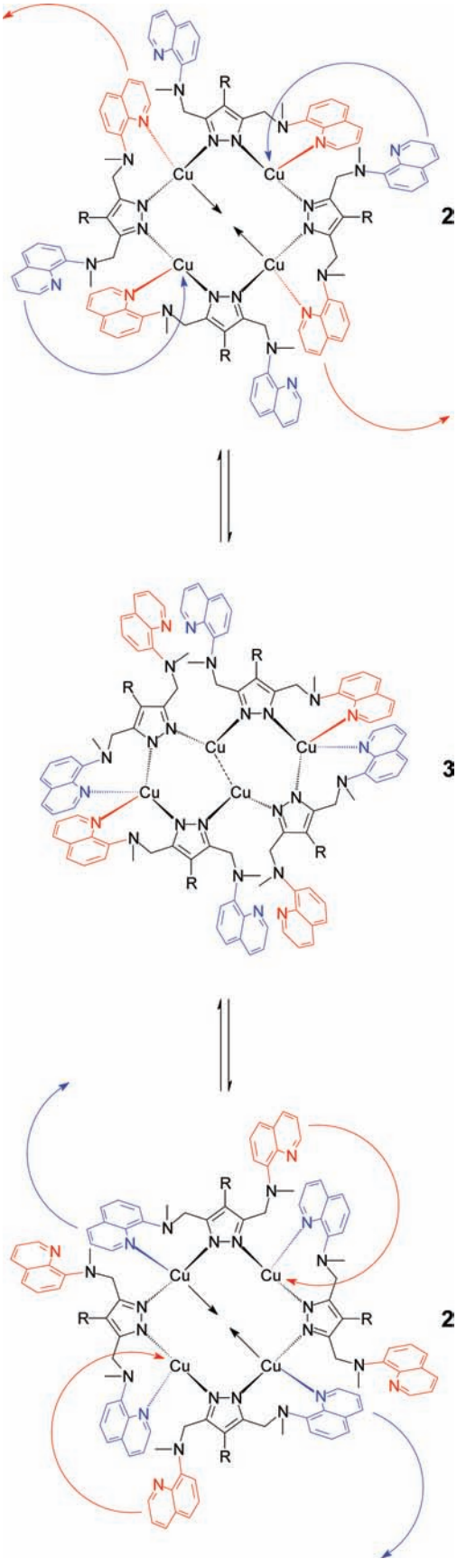

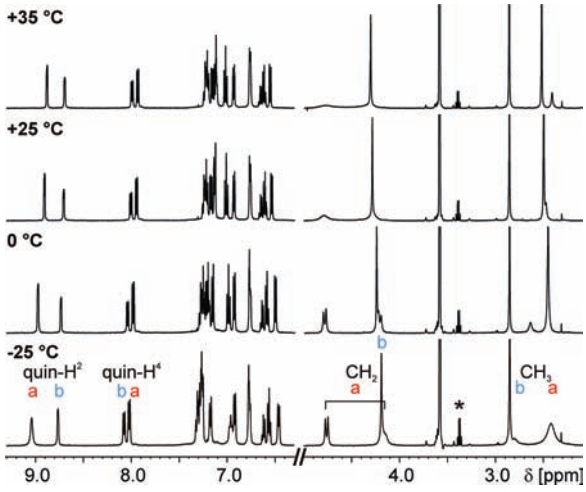

Figure 4. Variable-temperature ^{1}H NMR spectra of **3** (*denotes residual solvent signal).

process involving different oligomeric copper(I) pyrazolate species (see next paragraph).

Solution Behavior. 1−3 were studied by NMR spectroscopy in THF-d_8. Surprisingly, all three complexes show two sets of slowly (< 1 s^{-1}) exchanging NMR signals indicating the presence of two discrete species, hereafter termed **a** and **b**. While **a** is poorly populated in **1** (about 10%; the same ratio was found in benzene-d_6) its population reaches about 30% in **2** and 50% in **3**. In all cases, the ^{1}H and ^{13}C chemical shifts of both **a** and **b** differ only slightly (< 1 ppm for ^{13}C) from those of the free ligand, with substantial differences observed only for the Cu-coordinating pyrazolate core and the neighboring CH_2 groups. Furthermore and unlike in the crystal structure of **2** and **3**, the pyridyl/quinolyl side arms appear as equivalent. For example, the ^{1}H NMR signal belonging to the N-Me group appears as a narrow singlet that is shifted by about 0.1−0.4 ppm downfield in **b** relative to that in **a** in all complexes. A similar shift is observed for the signal of the pyrazolate-H^4 proton in **2**.

To relate the species **a** and **b** to the observations in the crystal structures, we recorded ^{1}H NMR spectra directly after dissolving single crystals of **2** and **3** in THF-d_8 at −50 °C. Although some signals appear very broad at this temperature, **a** was found highly enriched and was therefore assigned to a folded tetrameric (Cu-pz-)$_4$ species, presumably with the known S_4 symmetric backbone. This is also in agreement with the ^{1}H NMR signal assigned to the CH_2 protons in **a**, which at room temperature consists of two broad (50 Hz) peaks that become resolved into two AB doublets at −25 °C (Figure 4). Exchange between the two peaks thus amounts to about 150 s^{-1} and presumably arises from inversion of the (Cu-pz-)$_4$ core. Since the corresponding signal in **b** remains a narrow singlet down to −50 °C, we believe that **b** represents a planar (Cu-pz-)$_n$ structure.

To further investigate the association states of species **a** and **b**, we recorded ^{1}H DOSY NMR spectra that separate the signal sets by their diffusion coefficients D (Figure 5). For this purpose, dilute ($\approx$ 0.026 mM referring to monomeric Cu$\mathbf{L}^{1-3}$) solutions of all complexes as well as the free ligands $\mathbf{L}^{1-3}$H were prepared. The obtained diffusion coefficients were then converted into molecular radii r_H

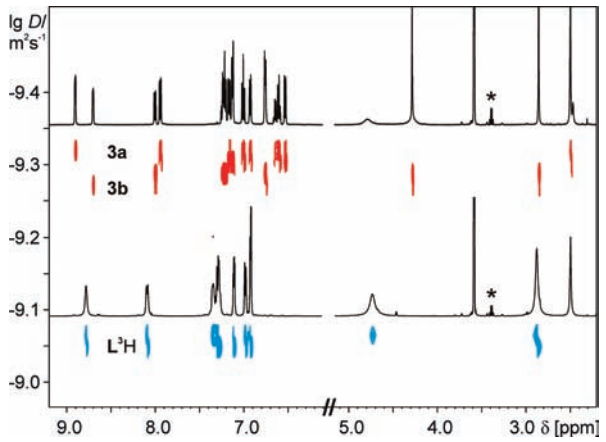

Figure 5. ^{1}H DOSY NMR spectrum of **3** overlaid by the spectrum of $\mathbf{L^3}$H (*denotes residual solvent signal).

using the Stokes−Einstein equation $D = k_BT/(6\pi\eta r_H)$ and the known viscosity η of THF of 0.48 cP at 25 °C[29] (Table 1).

Although the Stokes−Einstein equation is strictly valid only for spherical particles in a solvent continuum, the numbers clearly show that the size of the ligands increases from $\mathbf{L^2}$H to $\mathbf{L^3}$H and further to $\mathbf{L^1}$H. This is somewhat surprising in the latter case but presumably because of the additional CH_2 groups of $\mathbf{L^1}$H that lead to greater flexibility and potentially to a more space-filling arrangement of the ligand. The sizes of the complexes **1a**, **2a**, and **3a** are found at a constant ratio r_H(**a**)/r_H(**LH**) of 1.8, which is in agreement with the tetrameric complexes observed in the crystal structures. The ratio r_H(**b**)/r_H(**LH**) for the complexes **1b**, **2b**, and **3b** is substantially smaller (about 1.67) and therefore strongly supportive of a trimeric, planar (Cu-pz-)$_3$ structure (Chart 3) in analogy to a related silver pyrazolate complex where a similar behavior was observed.[30] One should note that our conclusions are based on the assumption that ligands are monomeric in THF solution. This seems reasonable: if ligands were dimeric, complexes (by comparing the DOSY data) would be octameric or hexameric (Cu_8 or Cu_6 species) instead of tetrameric or trimeric, which is very unlikely given that tetrameric or trimeric aggregates are the common motives observed in pyrazolate/Cu(I) chemistry.

An open question is still to what extent the pyridyl/quinolyl side arms coordinate to the copper centers of **1**−**3** in solution. As mentioned earlier, all ^{1}H and ^{13}C NMR signals from these arms appear as single narrow lines at room temperature, indicating fast conformational averaging. Only at −25 °C does the mobility start to slow down, as can be seen from a broadening of some ^{1}H signals of **1a**, **2a**, and **3a**, while the signals of **1b**, **2b**, and **3b** remain relatively narrow. Possibly, some of the adopted side arm conformations involve a transient interaction of N−CH_3, pyridyl, or quinolyl nitrogens with the copper centers. A tight binding of these donor atoms in solution is unlikely, however, since the observed ^{15}N chemical shifts in the complexes are generally too close (within ± 2 ppm) to that of the free ligands. The largest change was observed for the pyridine nitrogen of **1b**, which is shifted upfield by 4.7 ppm in benzene and 5.5 ppm in THF relative to the ligand $\mathbf{L^1}$H.

The absence of quinolyl-Cu interactions in solution is also corroborated by the similarity of the optical features related to the quinoline moieties of the free ligands and the complexes. Both $\mathbf{L^2}$H and $\mathbf{L^3}$H as well as complexes **2** and **3** show a relatively intense absorption band at around 355 nm (which is absent in $\mathbf{L^1}$H and **1**), and a broad emission with λ_{max} 467 nm ($\mathbf{L^3}$H, **2**) or 489 nm (**3**) upon excitation at λ_{ex} 360 nm (Figure 6 and Supporting Information, Figures S10−S12).

Table 1. Diffusion Coefficients and Molecular Radii Obtained from ^{1}H DOSY NMR

	1	**2**	**3**
D(**LH**) [10^{-10} m^{2}s^{-1}]	8.1 ± 0.2	9.6 ± 0.2	8.7 ± 0.2
D(**a**) [10^{-10} m^{2}s^{-1}]	4.6 ± 0.1	5.2 ± 0.1	4.8 ± 0.1
D(**b**) [10^{-10} m^{2}s^{-1}]	4.9 ± 0.1	5.8 ± 0.1	5.1 ± 0.1
r_H(**LH**) [Å]	5.9 ± 0.15	5.0 ± 0.1	5.5 ± 0.15
r_H(**a**) [Å]	10.5 ± 0.2	9.2 ± 0.2	10.0 ± 0.2
r_H(**b**) [Å]	9.8 ± 0.2	8.3 ± 0.2	9.3 ± 0.2
r_H(**a**)/r_H(**LH**)	1.78 ± 0.06	1.84 ± 0.06	1.82 ± 0.06
r_H(**b**)/r_H(**LH**)	1.67 ± 0.06	1.66 ± 0.06	1.69 ± 0.06
r_H(**a**)/r_H(**b**)	1.07 ± 0.03	1.11 ± 0.03	1.07 ± 0.03

Chart 3. Proposed Molecular Structures of **1b**−**3b** (with Fast Exchanging Side Arms)

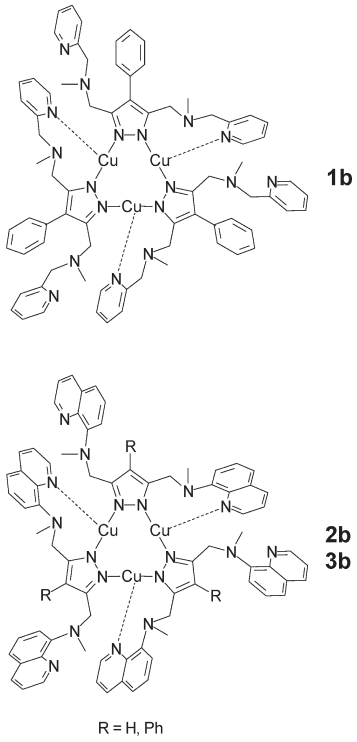

Conclusions

Three new potentially binucleating pyrazolate ligands with pyridyl- and quinolyl-side arms $\mathbf{L^{1-3}}$H were found to easily form oligonuclear homoleptic copper(I) pyrazolates **1**−**3** by clean reaction with mesitylcopper under elimination of mesitylene. In solution, two differently sized aggregates **a** and **b** of **2** and **3**, which are in slow exchange equilibrium at room temperature, are identified. Variable temperature ^{1}H NMR

(29) Lide, D. R. *Handbook of Chemistry and Physics*, 89th ed.; CRC Press: Boca Raton, FL, 2008.

(30) Scheele, U. J.; Georgiou, M.; John, M.; Dechert, S.; Meyer, F. *Organometallics* **2008**, *27*, 5146–5151.

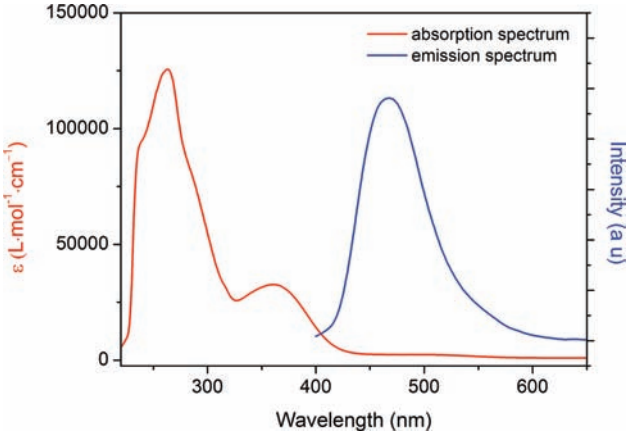

Figure 6. Absorption spectrum and normalized emission spectrum (λ_{ex} = 360 nm) of **2** at room temperature in THF solution.

and ^{1}H DOSY NMR spectra of both **2** and **3** are strongly supportive for the presence of a folded tetrameric (**a**) and planar trimeric (**b**) arrangement of the copper(I) pyrazolate core with weakly or non-bonding quinolyl side groups. Also in case of **1** a second species (a) occurs, but only in small amounts. Some features of the copper(I) pyrazolates observed in solution are displayed by the structures **2** and **3** elucidated by X-ray diffraction analysis, although both are substantially different: The molecular structure of **2** in the solid state represents a rare example of a tetrameric pyrazolate with trigonal-coordinated copper(I) centers involving weak interactions from four of the quinolyl side arms. Surprisingly, in comparison with **2**, complex **3** shows a partly rearranged structure that features a very rare cuprocuprate motif, supported by an intramolecular Cu···Cu contact. The solid state structure of **3** may be described as a snapshot of an intermediate along the pathway that interchanges bonding and non-bonding ligand side arms at the (Cu-pz-)$_4$ motif, interconverting two indistinguishable forms of **2**. This interconversion is proposed to proceed via sequential two-step attaching and detaching of two chelate side arms, initially at two opposite ligands of the Cu_4 arrangement, followed by the two remaining ligands, and concomitant with a square-rhomb-square distortion of the Cu_4 core. The rhomb-like intermediate is further stabilized by the intramolecular Cu···Cu (d^{10}-d^{10}) interaction. In solution, this interconversion is apparently very rapid, supporting the description of the ligand side arms as hemilabile sites that may rapidly bind to and detach from the metal ions. Attaching hemilabile chelating ligand side arms to the pyrazolate bridge may thus promote a new dynamic process of the (Cu-pz-)$_4$ motif that has not yet been described for related compounds with more simple pyrazolate ligands. It is obvious, however, that this intramolecular conversion should be viewed as part of a more complex scheme of dynamic processes, since in solution an equilibrium between tetrameric and trimeric (Cu-pz-) species, whose molecular structures are clearly different from the ones observed in solid state, is observed, and ligand side arms appear to be bonded to the metal ions only loosely or transiently at most.

NMR spectroscopic methods and X-ray diffraction analysis were found to be a powerful combination to get a deeper insight into structures and dynamics of these complex systems. Overall, pyrazolates with additional N-donating side arms represent valuable building blocks to form unique oligomeric copper(I) frameworks of high structural diversity and with potentially new dynamic behavior. Future work will focus on the photophysical properties of the present complexes and their derivatives, both in solution and in the solid state. Recent reports have shown that cyclic Cu^I pyrazolates may exhibit fascinating optical phenomena, including luminescence thermochromism, luminescence solvatochromism, concentration luminochromism, and so forth.[2] In the present set of complexes emissions may be related to both the side arm quinoline moieties as well as Cu···Cu interactions, which adds a further interesting aspect to the luminescence properties of this popular class of compounds.

Experimental Section

General Procedures. All manipulations involving copper organic compounds were carried out by using Schlenk techniques under an atmosphere of dry argon. Glassware and NMR tubes were dried with a heat gun under vacuum. Prior to use THF, diethyl ether, toluene, and pentane were freshly distilled from sodium/benzophenone. Benzene-d_6 and tetrahydrofurane-d_8 were distilled from sodium. Ethanol was dried according to the established method via sodium/diethyl phthalate.[31] 8-Aminoquinoline (Aldrich) and methyl iodide (Aldrich) were used as purchased. The syntheses of 3,5-bis(chloromethyl)-1-(tetrahydropyran-2-yl)pyrazole,[24b,25] 3,5-bis(chloromethyl)-1-(tetrahydropyran-2-yl)-4-phenylpyrazole[22] and **L^{1}H**[22] were described previously. Mesitylcopper was synthesized according to the known procedure.[32] Melting points were determined with a SRS (Stanford Research Systems) Opti Melt apparatus using open capillaries; the values are uncorrected. Elemental analyses were performed by the analytical laboratory of the Institute of Inorganic Chemistry at Georg-August-Universität Göttingen using an Elementar Vario EL III. NMR measurements were performed, unless indicated otherwise, at 25 °C on Bruker Avance 200, 300, and 500 spectrometers. ^{1}H and ^{13}C chemical shifts were calibrated internally to the solvent signals (7.24 and 77.0 ppm for $CDCl_3$, 7.15 and 128.0 ppm for C_6D_6, and 1.73 and 25.3 ppm for THF-d_8) and assigned using the following 2D experiments: COSY, NOESY (500 ms mixing), CH−COSY, and HMBC. ^{15}N chemical shifts were measured using a ^{15}N-HMQC (optimized for $^nJ_{HN}$ = 10 Hz) and calibrated indirectly to Ξ ($MeNO_2$) = 0.10136767. DOSY spectra were recorded with 2 ms bipolar *z*-gradient pulses ramped linearly from 1 to 50 G/cm and a diffusion delay of 70 ms. EI and FAB-MS-spectra were recorded on a Finnigan MAT 95. Values for *m*/*z* are given for the most intense peak of the isotope envelope. IR spectra were recorded using a Digilab Excalibur Series FTS 3000 spectrometer. UV−vis and fluorescence spectra of solutions of **1**−**3** in THF were measured with a Jasco V-50 UV−vis spectrometer and a Jasco FP-6200 fluorescence spectrometer.

8-(Aminomethyl)quinoline hydroiodide. The following procedure according to the literature method was used with modifications:[33] A solution of 8-aminoquinoline (5.040 g, 34.96 mmol) in ethanol (30 mL) was treated with methyl iodide (15.160 g, 106.81 mmol), refluxed for 9 h and then stored at −32 °C for 18 h. The red precipitate that had formed was filtered off and washed with small amounts of ethanol and diethyl ether. Recrystallization from ethanol (150 mL) gave an orange to red microcrystalline solid that was washed with diethyl ether

(31) Becker, H. G. O.; Berger, W.; Domschke, G.; Fanghänel, E.; Faust, J.; Fischer, M.; Gentz, F.; Gewald, K.; Gluch, R.; Mayer, R.; Müller, K.; Pavel, D.; Schmidt, H.; Schollberg, K.; Schwetlick, K.; Seiler, E.; Zeppenfeld, G. *Organikum*, 19nd ed.; Johann Ambrosius Barth Verlag GmbH: Leipzig, Berlin, Heidelberg, 1993; p 668 ff.
(32) Meyer, E. M.; Gambarotta, S.; Floriani, C.; Chiesi-Villa, A.; Guastini, C. *Organometallics* **1989**, *8*, 1067–1079.
(33) Deady, L. W.; Yusoff, N. I. *J. Heterocyclic Chem.* **1976**, *13*, 125–126.

and dried in vacuo for 90 min. Yield: 3.253 g (11.37 mmol, 33%). Anal. Calcd for $C_{10}H_{11}N_2I$ (286.11): C, 41.98; H, 3.88; N, 9.79. Found: C, 42.23; H, 3.97; N, 9.73. ^{1}H NMR (500.13 MHz, $CDCl_3$): δ 2.15 (s, 2 H, NH·HI), 3.08 (s, 3 H, CH_3), 7.02 (d, $^3J_{HH}$ = 8.0 Hz, 1 H, H^7), 7.30 (dd, $^3J_{HH}$ = 8.1 Hz, $^4J_{HH}$ = 0.6 Hz,1 H, H^5), 7.71 (t, $^3J_{HH}$ = 8.1 Hz, 1 H, H^6), 7.84 (dd, $^3J_{HH}$ = 5.3 Hz, $^3J_{HH}$ = 8.4 Hz, 1 H, H^3), 8.72 (dd, $^3J_{HH}$ = 8.4 Hz, $^4J_{HH}$ = 1.5 Hz, 1 H, H^4), 8.91 (dd, $^3J_{HH}$ = 5.3 Hz, $^4J_{HH}$ = 1.6 Hz, 1 H, H^2). ^{13}C NMR (75.48 MHz, $CDCl_3$): δ 30.0 (CH_3), 111.3 (CH, C^7), 114.4 (CH, C^5), 120.5 (CH, C^3), 128.4 (C, $C^{4a,8,8a}$), 130.4 (C, $C^{4a,8,8a}$), 131.7 (CH, C^6), 140.6 (CH, C^2), 141.1 (C, $C^{4a,8,8a}$), 146.0 (CH, C^4). MS (EI): *m*/*z* (rel. intensity) = 158 (100) $[M - HI]^+$, 144 (11) $[(C_9H_6N)NH_2]^+$, 130 (62) $[(C_9H_7N) + 2]^+$, 129 (54) $[(C_9H_7N) + 1]^+$, 128 (37) $[C_9H_7N]^+$.

L^{1}H.[22]. ^{1}H NMR (500.13 MHz, C_6D_6): δ 2.18 (s, 6 H, CH_3), 3.73 (s, 4 H, pz-CH_2), 3.76 (s, 4 H, py-CH_2), 6.58−6.61 (m, 2 H, py-C^5), 7.03−7.06 (m, 2 H, py-C^4), 7.07−7.12 (br, m, 2 H, py-C^3), 7.15−7.19 (m, 1 H, *p*-Ph), 7.30−7.33 (m, 2 H, *m*-Ph), 7.70−7.72 (m, 2 H, *o*-Ph), 8.38 (d, $^3J_{HH}$ = 4.6 Hz, 2 H, py-C^6). ^{1}H NMR (500.13 MHz, THF-d_8): δ 2.18 (s, 6 H, CH_3), 3.62 (s, 4 H, pz-CH_2), 3.67 (s, 4 H, py-CH_2), 7.09 (dd, $^3J_{HH}$ = 7.5 Hz, $^3J_{HH}$ = 5.0 Hz, 2 H, py-C^5), 7.22 (tt, $^3J_{HH}$ = 7.4 Hz, $^4J_{HH}$ = 1.2 Hz, 1 H, *p*-Ph), 7.31−7.35 (m, 4 H, py-C^3, *m*-Ph), 7.56 (dt, $^3J_{HH}$ = 7.7 Hz, $^4J_{HH}$ = 1.8 Hz, 2 H, py-C^4), 7.61 (d, $^3J_{HH}$ = 7.7 Hz, 2 H, *o*-Ph), 8.41 (d, $^3J_{HH}$ = 4.8 Hz, 2 H, py-C^6). ^{13}C NMR (125.77 MHz, C_6D_6): δ 42.5 (CH_3), 52.7 (CH_2, pz-CH_2), 62.8 (CH_2, py-CH_2), 120.5 (C, pz-C^4), 121.8 (CH, py-C^5), 123.3 (CH, py-C^3), 126.3 (CH, *p*-Ph), 128.5 (CH, *m*-Ph), 130.4 (CH, *o*-Ph), 134.8 (C, *i*-Ph), 136.0 (CH, py-C^4), 143.2 (br, C, pz-$C^{3,5}$), 149.1 (CH, py-C^6), 159.8 (C, py-C^2). ^{13}C NMR (125.77 MHz, THF-d_8): δ 42.5 (CH_3), 53.5 (CH_2, pz-CH_2), 63.8 (CH_2, py-CH_2), 120.7 (C, pz-C^4), 122.4 (CH, py-C^5), 123.6 (CH, py-C^3), 126.6 (CH, *p*-Ph), 128.8 (CH, *m*-Ph), 130.8 (CH, *o*-Ph), 135.3 (C, *i*-Ph), 136.7 (CH, py-C^4), 143.5 (br, C, pz-$C^{3,5}$), 149.5 (CH, py-C^6), 160.7 (C, py-C^2). ^{15}N NMR (50.69 MHz, C_6D_6): δ −343.4 (H_3C−N), −65.2 (py-N). The pyrazole-N resonance is too broad to be detected. ^{15}N NMR (50.69 MHz, THF-d_8): δ −343.5 (H_3C−N), −63.3 (py-N). The pyrazole-N resonance is too broad to be detected.

L^{2}H. The compound was prepared according to the method described for **L^{1}H** by the use of Na_2CO_3 (4.770 g, 45.00 mmol), 3,5-bis(chloromethyl)-1-(tetrahydropyran-2-yl)pyrazole (1.120 g, 4.50 mmol), and 8-(aminomethyl)quinoline hydroiodide (2.570 g, 8.98 mmol). The brownish yellow crude product was purified by column chromatography (bas. Al_2O_3, ethyl acetate/pentane 1:1). Yield: 1.060 g (2.59 mmol, 58%). Mp: 126 °C. Anal. Calcd for $C_{25}H_{24}N_6$: C, 73.51; H, 5.92; N, 20.57. Found: C, 73.34; H, 6.00; N, 20.62. ^{1}H NMR (300.13 MHz, THF-d_8): δ 2.91 (s, 6 H, CH_3), 4.74 (br s, 4 H, CH_2), 6.00 (s, 1 H, pz-H^4), 7.03 (dd, $^4J_{HH}$ = 1.8 Hz, $^3J_{HH}$ = 7.1 Hz, 2 H, quin-H^7), 7.32 (dd, $^4J_{HH}$ = 1.8 Hz, $^3J_{HH}$ = 8.1 Hz, 2 H, quin-H^5), 7.35−7.41 (m, 4 H, quin-$H^{3,6}$), 8.15 (dd, $^4J_{HH}$ = 1.8 Hz, $^3J_{HH}$ = 8.3 Hz, 2 H, quin-H^4), 8.84 (dd, $^4J_{HH}$ = 1.8 Hz, $^3J_{HH}$ = 4.1 Hz, 2 H, quin-H^2). ^{13}C NMR (125.77 MHz, THF-d_8): δ 39.9 (CH_3), 53.6 (br, CH_2), 104.6 (CH, pz-C^4), 116.0 (CH, quin-C^7), 120.3 (CH, quin-C^5), 121.5 (CH, quin-C^3), 127.5 (CH, quin-C^6), 130.9 (C, quin-C^{4a}), 137.1 (CH, quin-C^4), 143.5 (C, quin-C^{8a}), 147.8 (CH, quin-C^2), 150.0 (C, quin-C^8). The pyrazole-$C^{3,5}$ carbon atoms appear as extremely broad resonance at 147 ppm. ^{15}N NMR (50.69 MHz, THF-d_8): δ −325.5 (H_3C−N), −71.5 (quin-N). The pyrazole-N resonance is too broad to be detected. MS (EI): *m*/*z* (rel. intensity) = 409.2 (3) $[M + 1]^+$, 408.2 (10) $[M]^+$, 251.1 (17) $[M - C_{10}H_9N_2]^+$, 250.1 (100) $[M - C_{10}H_9N_2 - 1]^+$, 158.0 (35) $[C_{10}H_9N_2 + 1]^+$, 157.0 (49) $[C_{10}H_9N_2]^+$, 129 (23) $[C_9H_6N + 1]^+$, 128 (5) $[C_9H_6N]^+$. IR (KBr, cm^{-1}): 3275, 3102, 3086, 3057, 3046, 2980, 2943, 2872, 2853, 2789, 1607, 1595, 1568, 1501, 1474, 1454, 1435, 1418, 1389, 1366, 1354, 1304, 1285, 1246, 1211, 1179, 1159, 1128, 1121, 1082, 1053, 1032, 1024, 1001, 961, 922, 912, 822, 791, 781, 752, 741, 710, 683, 669, 646, 619, 594, 581, 548, 459. UV−vis (CH_2Cl_2): λ [nm] (ε [L·mol^{-1}·cm^{-1}]) 260 (19520), 353 (4030).

L^{3}H. A suspension of anhydrous Na_2CO_3 (5.306 g, 50.06 mmol), 3,5-bis(chloromethyl)-1-(tetrahydropyran-2-yl)-4-phenylpyrazole (1.638 g, 5.04 mmol), and 8-(aminomethyl)-quinoline hydroiodide (2.882 g, 10.07 mmol) in acetonitrile (250 mL) was refluxed for 10 d, then filtered and evaporated to dryness. The remaining salts were removed by extracting the brownish residue with CH_2Cl_2 (50 mL). After evaporation of all volatile materials in vacuo, the resulting solid was dissolved in dry ethanol (20 mL) and treated with ethanolic HCl (40 wt %, 10 mL). The formation of the hydrochloride salt as an orange precipitate was completed after stirring for 2 h and addition of diethyl ether (50 mL). It was filtered, washed with diethyl ether (4 × 5 mL), and dried in vacuo for 3 h. Treating with aqueous NaOH (pH 12, 60 mL) gave a light brown precipitate that was filtered, washed with water (6 × 50 mL), and dried in vacuo for 12 h. The brownish crude product was purified by column chromatography (bas. Al_2O_3, THF) to yield a citreous yellow powder. Yield: 1.322 g (2.73 mmol, 54%). Mp: 93 °C. Anal. Calcd for $C_{31}H_{28}N_6 \cdot 0.15\ CH_2Cl_2$: C, 75.23; H, 5.74; N, 16.90. Found: C, 75.17; H, 5.85; N, 16.67. ^{1}H NMR (500.13 MHz, THF-d_8): δ 2.88 (br s, 6 H, CH_3), 4.73 (br s, 4 H, CH_2), 6.92−6.94 (m, 3 H, *p*-Ph, *m*-Ph), 6.99 (dd, $^4J_{HH}$ = 1.9 Hz, $^3J_{HH}$ = 7.0 Hz, 2 H, quin-H^7), 7.10−7.12 (m, 2 H, *o*-Ph), 7.27−7.32 (m, 4 H, quin-$H^{5,6}$), 7.35 (dd, $^3J_{HH}$ = 4.1 Hz, $^3J_{HH}$ = 8.2 Hz, 2 H, quin-H^3), 8.10 (dd, $^4J_{HH}$ = 1.5 Hz, $^3J_{HH}$ = 8.2 Hz, 2 H, quin-H^4), 8.78−8.79 (m, 2 H, quin-H^2). ^{13}C NMR (125.77 MHz, THF-d_8): δ 40.5 (br, CH_3), 51.8 (br, CH_2), 116.6 (CH, quin-C^7), 120.6 (CH, quin-C^5), 120.9 (C, pz-C^4), 121.5 (CH, quin-C^3), 126.3 (CH, *p*-Ph), 127.3 (CH, quin-C^6), 128.3 (CH, *m*-Ph), 130.7 (CH, *o*-Ph), 130.8 (C, quin-C^{4a}), 134.4 (C, *i*-Ph), 137.0 (CH, quin-C^4), 143.7 (C, quin-C^{8a}), 147.8 (br, CH, quin-C^2), 150.1 (C, quin-C^8). The pyrazole-$C^{3,5}$ carbon atoms appear as an extremely broad resonance at 148 ppm. ^{15}N NMR (50.69 MHz, THF-d_8): δ −326.2 (H_3C−N), −72.5 (quin-N). The pyrazole-N resonance is too broad to be detected. MS (EI): *m*/*z* (rel. intensity) = 484 (8) $[M]^+$, 327 (23) $[M - C_{10}H_9N_2]^+$, 326 (92) $[M - C_{10}H_9N_2 - 1]^+$, 311 (18) $[M - C_{11}H_{12}N_2 - 1]^+$, 157 (100) $[C_{10}H_9N_2]^+$, 129 (59) $[C_9H_6N + 1]^+$, 128 (14) $[C_9H_6N]^+$. IR (KBr, cm^{-1}): 3263, 3053, 3030, 2940, 2884, 2851, 2791, 1607, 1595, 1566, 1501, 1472, 1447, 1420, 1389, 1368, 1354, 1314, 1292, 1240, 1175, 1117, 1078, 1059, 1032, 1011, 995, 920, 847, 826, 791, 750, 700, 667, 594, 583, 555, 544, 473, 461. UV−vis (CH_2Cl_2): λ [nm] (ε [L·mol^{-1}·cm^{-1}]) 220 (15130), 260 (19690), 353 (3920).

Complex 1. A solution of mesitylcopper (104 mg including 0.06 equiv of toluene, determined by ^{1}H NMR, 0.55 mmol) in THF (10 mL) was treated dropwise with a solution of **L^{1}H** (227 mg, 0.55 mmol) in THF (10 mL) at −78 °C. After stirring at room temperature overnight, the solution was filtered, concentrated to approximately 5 mL, and layered with diethyl ether (3−4 mL). The microcrystalline solid that had formed after several days at +4 °C was removed by filtration, washed first with toluene in portions (5 mL), then 3-fold with pentane (3 × 2 mL), and dried for 14 h in vacuo. Yield: 174 mg of a citreous yellow powder (0.37 mmol, 67%). Anal. Calcd for $C_{100}H_{108}N_{24}Cu_4$: C, 63.21; H, 5.73; N, 17.69. Found: C, 62.89; H, 5.69; N, 17.48. ^{1}H NMR (500.13 MHz, C_6D_6): δ 2.17 (br s, 6 H, CH_3, **1a**), 2.23 (s, 6 H, CH_3, **1b**), 3.65 (s, 4 H, py-CH_2, **1b**), 3.69 (br s, 2 H, pz-CH_2, **1a**), 3.95 (s, 4 H, pz-CH_2, **1b**), 6.50−6.53 (m, 2 H, py-C^5), 6.95−6.97 (m, 4 H, py-$C^{3,4}$), 7.21 (tt, $^3J_{HH}$ = 7.4 Hz, $^4J_{HH}$ = 1.2 Hz, 1 H, *p*-Ph, **1b**), 7.29 (br t, $^3J_{HH}$ = 7.5 Hz, 2 H, *m*-Ph, **1a**), 7.37 (t, $^3J_{HH}$ = 7.5 Hz, 2 H, *m*-Ph, **1b**), 7.67 (br d, $^3J_{HH}$ = 7.4 Hz, 2 H, *o*-Ph, **1a**), 7.70 (d, $^3J_{HH}$ = 7.4 Hz, 2 H, *o*-Ph, **1b**), 8.39 (br d, $^3J_{HH}$ = 4.8 Hz, 2 H, py-C^6, **1a**), 8.47 (d, $^3J_{HH}$ = 4.8 Hz, 2 H, py-C^6, **1b**). The remaining signals of **1a** are hidden under that of **1b**. ^{1}H NMR (500.13 MHz, THF-d_8): δ 2.05 (br s, 6 H, CH_3, **1a**), 2.24 (s, 6 H, CH_3, **1b**), 3.51 (br s, 2 H, pz-CH_2, **1a**), 3.61

(s, 4 H, py-CH_2, **1b**), 3.88 (s, 4 H, pz-CH_2, **1b**), 6.91 (dd, $^3J_{HH}$ = 7.2 Hz, $^3J_{HH}$ = 5.0 Hz, 2 H, py-C^5, **1b**), 6.95−6.97 (br m, 2 H, py-C^5, **1a**), 7.14 (d, $^3J_{HH}$ = 7.7 Hz, 2 H, py-C^3, **1b**), 7.19 (t, $^3J_{HH}$ = 7.4 Hz, 1 H, *p*-Ph, **1b**), 7.32 (t, $^3J_{HH}$ = 7.6 Hz, 2 H, *m*-Ph, **1b**), 7.37 (dt, $^3J_{HH}$ = 7.6 Hz, $^4J_{HH}$ = 1.6 Hz, 2 H, py-C^4, **1b**), 7.41 (br d, $^3J_{HH}$ = 7.4 Hz, 2 H, *o*-Ph, **1a**), 7.52 (d, $^3J_{HH}$ = 7.4 Hz, 2 H, *o*-Ph, **1b**), 8.32−8.33 (br m, 2 H, py-C^6, **1a**) 8.37 (d, $^3J_{HH}$ = 4.2 Hz, 2 H, py-C^6, **1b**). The remaining signals of **1a** are hidden under that of **1b**. ^{13}C NMR (125.77 MHz, C_6D_6): δ 43.3 (CH_3), 55.7 (CH_2, pz-CH_2), 63.2 (CH_2, py-CH_2), 118.9 (C, pz-C^4), 121.8 (CH, py-C^5), 123.0 (CH, py-C^3), 125.5 (CH, *p*-Ph), 128.3 (CH (overlapped by benzene signal), *m*-Ph), 130.3 (CH, *o*-Ph), 135.9 (CH, py-C^4), 136.5 (C, *i*-Ph), 147.2 (C, pz-$C^{3,5}$), 149.2 (CH, py-C^6), 160.2 (C, py-C^2), all from **1b**. Signals of **1a** are beyond detection. ^{13}C NMR (125.77 MHz, THF-d_8): δ 43.5 (CH_3), 55.9 (CH_2, pz-CH_2), 63.6 (CH_2, py-CH_2), 119.6 (C, pz-C^4), 122.5 (CH, py-C^5), 123.6 (CH, py-C^3), 125.9 (CH, *p*-Ph), 128.5 (CH, *m*-Ph), 130.7 (CH, *o*-Ph), 136.6 (CH, py-C^4), 136.7 (C, *i*-Ph), 147.8 (C, pz-$C^{3,5}$), 149.6 (CH, py-C^6), 160.6 (C, py-C^2), all from **1b**. Signals of **1a** are beyond detection. ^{15}N NMR (50.69 MHz, C_6D_6): δ −341.0 (H_3C−N), −119.6 (pz-N), −69.9 (py-N), all from **1b**. Signals of **1a** are beyond detection.^{15}N NMR (50.69 MHz, THF-d_8): δ −341.5 (H_3C−N), −121.2 (pz-N), −68.8 (py-N), all from **1b**. Signals of **1a** are beyond detection. MS (FAB in 3-NBA): *m*/*z* (rel. intensity) = 1485.6 (2) $[M - (C_{25}H_{27}N_6)]^+$, 1011.2 (12) $[(C_{25}H_{27}N_6)_2Cu_3]^+$, 948.3 (11) $[(C_{25}H_{27}N_6)_2Cu_2]^+$, 537.1 (100) $[(C_{25}H_{27}N_6)Cu_2]^+$. IR (KBr, cm^{-1}): 3069, 3051, 3019, 3013, 2974, 2940, 2876, 2835, 2793, 1603, 1589, 1570, 1545, 1474, 1452, 1433, 1364, 1335, 1310, 1194, 1119, 1047, 1024, 1016, 995, 970, 955, 887, 868, 851, 762, 756, 702, 633, 613, 584, 523, 490, 473, 459. UV−vis (THF): λ [nm] (ε [$L \cdot mol^{-1} \cdot cm^{-1}$]) 258 (37150).

Complex 2. A solution of mesitylcopper (92 mg, 0.49 mmol, see **1**) in toluene (10 mL) was treated with a solution of $\mathbf{L^2}$H (199 mg, 0.49 mmol) in toluene (10 mL) at −78 °C by means of a cannula. After stirring at room temperature overnight, the reaction mixture was concentrated to 3 mL. The yellow precipitate formed was removed by filtration, washed twice with toluene (2 × 2 mL), then 3-fold with pentane (3× 5 mL) and was dried in vacuo for 14 h. Yield: 166 mg of a yellow microcrystalline solid (0.35 mmol, 71%). Anal. Calcd for $C_{100}H_{92}N_{24}Cu_4$: C, 63.75; H, 4.92; N, 17.84. Found: C, 63.80; H, 5.28; N, 17.20. ^{1}H NMR (500.13 MHz, THF-d_8): δ 2.57 (s, 6 H, CH_3, **2a**), 2.80 (s, 6 H, CH_3, **2b**), 4.41 (s, 4 H, CH_2, **2b**), 4.65 (br s, 4 H, CH_2, **2a**), 5.69 (s, pz-H^4, **2a**), 5.91 (s, pz-H^4, **2b**), 6.83 (d, $^3J_{HH}$ = 6.2 Hz, 2 H, quin-H^7, **2b** and 2 H, **2a**), 7.18−7.26 (m, 6 H, quin-$H^{3,5,6}$, **2b** and 6 H, **2a**), 7.99 (dd, $^4J_{HH}$ = 1.6 Hz, $^3J_{HH}$ = 8.3 Hz, 2 H, quin-H^4, **2b**), 8.01−8.02 (m, 2 H, quin-H^4, **2a**, overlaid by the signal of **2b**), 8.70 (dd, $^4J_{HH}$ = 1.6 Hz, $^3J_{HH}$ = 4.0 Hz, 2 H, quin-H^2, **2b**), 8.84 (dd, $^4J_{HH}$ = 1.6 Hz, $^3J_{HH}$ = 4.0 Hz, 2 H, quin-H^2, **2a**). ^{13}C NMR (125.77 MHz, THF-d_8): δ 40.0 (CH_3, **2a**), 40.4 (CH_3, **2b**), 55.4 (CH_2, **2b**), 55.5 (CH_2, **2a**), 103.1 (CH, pz-C^4, **2a**), 103.5 (CH, pz-C^4, **2b**), 116.1 (CH, quin-C^7, **2a**), 116.4 (CH, quin-C^7, **2b**), 120.2 (CH, quin-C^5, **2a**), 120.6 (CH, quin-C^5, **2b**), 121.4 (CH, quin-C^3, **2b**), 121.5 (CH, quin-C^3, **2a**), 127.2 (CH, quin-C^6, **2b**), 127.3 (CH, quin-C^6, **2a**), 130.6 (C, quin-C^{4a}, **2a**), 130.7 (C, quin-C^{4a}, **2b**), 136.7 (CH, quin-C^4, **2a**, **2b**), 143.4 (C, quin-C^{8a}, **2a**), 143.6 (C, quin-C^{8a}, **2b**), 148.1 (CH, quin-C^2, **2b**), 148.3 (CH, quin-C^2, **2a**), 150.1 (C, quin-C^8, **2a**), 150.1 (C, quin-C^8, **2b**), 151.2 (C, pz-$C^{3,5}$, **2a**), 152.4 (C, pz-$C^{3,5}$, **2b**). ^{15}N NMR (50.69 MHz, THF-d_8): δ −325.3 (H_3C−N, **2b**), −128.5 (pz-N, **2b**), −126.1 (pz-N, **2a**), −72.3 (quin-N, **2a**), −71.2 (quin-N, **2b**). The H_3C−N resonance in **2a** is too weak to be detected. MS (FAB in 3-NBA): *m*/*z* (rel. intensity) = 1473.5 (3) $[M - (C_{25}H_{23}N_6)]^+$, 1003.2 (3) $[(C_{25}H_{23}N_6)_2Cu_3]^+$, 940.2 (6) $[(C_{25}H_{23}N_6)_2Cu_2]^+$, 535.0 (100) $[(C_{25}H_{23}N_6)Cu_2 + 2]^+$, 533.0 (90) $[(C_{25}H_{23}N_6)Cu_2]^+$. IR (KBr, cm^{-1}): 3046, 3032, 2947, 2847, 2783, 1915, 1607, 1595, 1566, 1501, 1468, 1449, 1418, 1389, 1366, 1352, 1331, 1296, 1240, 1209, 1192, 1175, 1119, 1080, 1057, 1047, 1032, 970, 924, 847, 824, 806, 789, 750, 708, 681, 656, 604, 579, 548, 525, 511, 459. UV−vis (THF): λ [nm] (ε [$L \cdot mol^{-1} \cdot cm^{-1}$]) 263 (125660), 361 (32660).

Table 2. Crystal Data and Refinement Details for **2** and **3**

	2	**3**
formula	$C_{100}H_{92}Cu_4N_{24}$	$C_{124}H_{108}Cu_4N_{24} \cdot 3C_7H_8$
M_r	1884.14	2464.91
crystal size [mm]	0.13 × 0.10 × 0.08	0.20 × 0.04 × 0.02
crystal system	tetragonal	triclinic
space group	$I4_1/a$	$P\bar{1}$
a [Å], α [deg]	14.2010(3), 90	15.7778(5), 104.105(2)
b [Å], *β* [deg]	14.2010(3), 90	18.3074(7), 93.087(2)
c [Å], *γ* [deg]	50.9312(19), 90	24.0587(8), 115.284(2)
V [Å^3]	10271.2(5)	5994.5(4)
Z	4	2
$\rho_{calcd.}$ [g cm^{-3}]	1.218	1.366
F(000)	3904	2572
μ [mm^{-1}]	0.872	1.306
T_{max}/T_{min}		0.9743/0.7801
hkl range	−14 +16, ± 16, ± 59	±17, −20 +19, 0 +27
θ range [deg]	1.49 − 24.43	1.92 − 60.87
measured refl.	26802	101071
unique refl. [R_{int}]	4253 [0.1270]	16908 [0.0803]
observed refl.	$I > 2\sigma(I)$ 2820	$I > 2\sigma(I)$ 12603
data/restraints/param.	4253/11/258	16908/2024/1697
goodness-of-fit	1.054	1.045
*R*1 ($I > 2\sigma(I)$)	0.0756	0.0579
*wR*2 (all data)	0.1579	0.1683
resid. el. dens. [e Å^{-3}]	0.465/−0.464	0.888/−0.570

Complex 3. A solution of mesitylcopper (92 mg, 0.49 mmol, see **1**) in toluene (10 mL) was treated with a solution of $\mathbf{L^3}$H (237 mg, 0.49 mmol) in toluene (10 mL) at −78 °C by means of a cannula. After stirring at room temperature overnight, the reaction mixture was filtered, concentrated to 5 mL, and stored at +4 °C to give orange needles that were collected by filtration, washed with toluene (3 × 2 mL), pentane (5 × 5 mL) and dried in vacuo for 15 h. Yield: 234 mg of an orange microcrystalline solid (0.36 mmol, 73%).[34] Anal. Calcd for $C_{124}H_{108}N_{24}Cu_4 \cdot 1.11C_7H_8$: C, 69.09; H, 5.14; N, 14.67. Found: C, 69.35; H, 5.32; N, 14.08.

^{1}H NMR (500.13 MHz, THF-d_8): δ 2.50 (s, 6 H, CH_3, **3a**), 2.86 (s, 6 H, CH_3, **3b**), 4.28 (s, 4 H, CH_2, **3b**, and 2 H, **3a**), 4.79 (br s, 2 H, CH_2, **3a**), 6.54 (d, $^3J_{HH}$ = 7.6 Hz, 2 H, quin-H^7, **3a**), 6.59−6.62 (m, 2 H, *m*-Ph, **3a**), 6.63−6.67 (m, 1 H, *p*-Ph, **3a**), 6.75−6.77 (m, 5 H, quin-H^7, *m*-, *p*-Ph, **3b**), 6.92−6.94 (m, 2 H, *o*-Ph, **3a**), 7.01 (t, $^3J_{HH}$ = 7.8 Hz, 2 H, quin-H^6, **3a**), 7.12−7.14 (m, 2 H, quin-H^5, **3a** and 2 H, *o*-Ph, **3b**), 7.17 (dd, $^3J_{HH}$ = 4.2 Hz, $^3J_{HH}$ = 8.2 Hz, 2 H, quin-H^3, **3a**), 7.20−7.26 (m, 6 H, quin-$H^{3,5,6}$, **3b**), 7.95 (dd, $^4J_{HH}$ = 1.7 Hz, $^3J_{HH}$ = 8.3 Hz, 2 H, quin-H^4, **3a**), 8.00 (dd, $^4J_{HH}$ = 1.8 Hz, $^3J_{HH}$ = 8.3 Hz, 2 H, quin-H^4, **3b**), 8.71 (dd, $^4J_{HH}$ = 1.8 Hz, $^3J_{HH}$ = 4.1 Hz, 2 H, quin-H^2, **3b**), 8.91 (dd, $^4J_{HH}$ = 1.8 Hz, $^3J_{HH}$ = 4.2 Hz, 2 H, quin-H^2, **3a**). ^{13}C NMR (125.77 MHz, THF-d_8): δ 40.2 (CH_3, **3a**), 41.2 (CH_3, **3b**), 53.6 (CH_2, **3b**), 54.0 (CH_2, **3a**), 116.2 (CH, quin-C^7, **3a**), 117.5 (CH, quin-C^7, **3b**), 119.8 (C, pz-C^4, **3a**), 119.8 (C, pz-C^4, **3b**), 120.1 (CH, quin-C^5, **3a**), 121.1 (CH, quin-C^5, **3b**), 121.4 (CH, quin-C^3, **3a**), 121.5 (CH, quin-C^3, **3b**), 125.1 (CH, *p*-Ph, **3a**), 125.5 (CH, *p*-Ph, **3b**), 127.0 (CH, quin-C^6, **3a**), 127.2 (CH, quin-C^6, **3b**), 127.7 (CH, *m*-Ph, **3a**), 127.8 (CH, *m*-Ph, **3b**), 130.5 (CH, *o*-Ph, **3a**), 130.6 (C, quin-C^{4a}, **3a**), 130.7 (C, quin-C^{4a}, **3b**), 130.8 (CH, *o*-Ph, **3b**), 135.4 (C, *i*-Ph, **3a**), 135.6 (C, *i*-Ph, **3b**), 136.5 (CH, quin-C^4, **3a**), 136.6 (CH, quin-C^4, **3b**), 143.4 (C, quin-C^{8a}, **3a**), 143.8 (C, quin-C^{8a}, **3b**), 147.2 (C, pz-$C^{3,5}$, **3a**), 148.0 (C, pz-$C^{3,5}$, **3b**), 148.3 (br, CH, quin-C^2, **3b**), 148.6 (br, CH, quin-C^2, **3a**), 150.3 (C, quin-C^8, **3a**), 150.6 (C, quin-C^8, **3b**).

(34) Albeit toluene-free material of **3** could be isolated, a satisfactory elemental analysis was obtained only from the toluene-containing charge. Toluene molecules are also found in the crystal structure of **3**.

^{15}N NMR (50.69 MHz, THF-d_8): δ −326.0 (H_3C−N, **3b**), −323.9 (H_3C−N, **3a**), −121.8 (pz-N, **3b**), −74.4 (quin-N, **3b**), −74.2 (quin-N, **3a**). The pyrazole-N resonance in **3a** cannot be detected as the CH_2 proton signal is broad. MS (FAB in 3-NBA): m/z (rel. intensity) = 2249.7 (1) $[M + Cu + 2]^+$, 1701.5 (8) $[M - (C_{31}H_{27}N_6)]^+$, 1155.2 (5) $[(C_{31}H_{27}N_6)_2Cu_3]^+$, 1092.2 (5) $[(C_{31}H_{27}N_6)_2Cu_2]^+$, 611.0 (100) $[(C_{31}H_{27}N_6)Cu_2 + 2]^+$, 545.1 (8) $[(C_{31}H_{27}N_6)Cu - 1]^+$. IR (KBr, cm^{-1}): 3046, 2947, 2845, 2785, 1942, 1915, 1603, 1566, 1543, 1501, 1470, 1447, 1418, 1387, 1366, 1348, 1325, 1261, 1236, 1190, 1173, 1119, 1080, 1053, 1034, 1018, 999, 978, 924, 822, 789, 748, 700, 679, 665, 652, 646, 606, 594, 577, 565, 546, 513, 459. UV−vis (THF): λ [nm] (ε [$L \cdot mol^{-1} \cdot cm^{-1}$]) 236 (47040), 259 (52360), 315 (13180), 350 (10910).

X-ray Crystallography. X-ray data for complex **2** (Table 2) were collected on a STOE IPDS II diffractometer (graphite monochromated Mo Kα radiation, λ = 0.71073 Å) by use of ω scans at −140 °C (Table 1). The structure was solved by direct methods and refined on F^2 using all reflections with SHELX-97.[35] The non-hydrogen atoms were refined anisotropically, except those in disordered parts. Hydrogen atoms were placed in calculated positions and assigned to an isotropic displacement parameter of 0.08 Å^2. In the structure of **2** one quinoline side arm was found to be disordered about two positions (occupancy factors 0.566(14)/0.434(14)). SADI ($d_{N-C(quinoline)}$) and DFIX ($d_{C=C}$ = 1.39 Å, $d_{C=N}$ = 1.34 Å) restraints were used to model the disorder. For the toluene solvent molecules in **2** no satisfactory model for the disorder could be found, and for further refinement the contribution of the missing solvent molecules (1975.6 Å^3, electron count 449) was subtracted from the reflection data by the SQUEEZE[36] routine of the PLATON program[37]. X-ray data for complex **3** were collected on a Bruker three circle diffractometer with a SMART 6000 detector and Cu Kα radiation (λ = 1.54178 Å) at 100 K. In the non-meroedric twinned crystal two cell domains were discovered with the program CELL_NOW[38] and corrected and detwinned with the TWINABS[39] program. A twin ratio of 0.620(1):0.380(1) was calculated. The structure was solved using direct methods and refined by full-matrix least-squares procedures against F^2 with SHELX-97.[35] Non-hydrogen atoms were refined anisotropically, and hydrogen atoms were added using the riding model. Two toluene molecules are disordered with an occupancy of 0.80 and 0.20 and form solvent clusters.

Acknowledgment. We are grateful to Annette Meiners for experimental contributions to the preparation of $\mathbf{L^2}$H. Financial support by the Fonds der Chemischen Industrie is gratefully acknowledged.

Supporting Information Available: CIF files, molecule plots, tables of all bond lengths, angles, and atomic coordinates for the structures of the complexes **1** and **2**. Variable temperature ^{1}H NMR spectra of **1** and **2**. ^{1}H DOSY spectra of $\mathbf{L^1}$H, $\mathbf{L^2}$H, **1**, and **2**. ^{15}N HMQC spectra of $\mathbf{L^{1-3}}$H and **1**−**3**. This material is available free of charge via the Internet at http://pubs.acs.org.

(35) (a) Sheldrick, G. M. *SHELXL-97, Program for Crystal Structure Refinement*; University of Göttingen: Göttingen, Germany, 1997. (b) Sheldrick, G. M. *SHELXS-97, Program for Crystal Structure Solution*; University of Göttingen: Göttingen, Germany, 1997. (c) Sheldrick, G. M. *Acta Crystallogr.* **2008**, *A64*, 112–122.

(36) v. d. Sluis, P.; Spek, A. L. *Acta Crystallogr.* **1990**, *A46*, 194–201.

(37) Spek, A. L. *PLATON, A Multipurpose Crystallographic Tool*; Utrecht University: Utrecht, The Netherlands, 2003.

(38) Sheldrick, G. M. *CELL_NOW*; University of Göttingen: Göttingen, Germany, 2005.

(39) Sheldrick, G. M. *TWINABS, Program for Performing Absorption Corrections to X-ray Diffraction Patterns Collected from Non-Merohedrally Twinned and Multiple Crystals*; University of Göttingen: Göttingen, Germany, 2002.